PAPER

Check for updates

Combination of practical and theoretical measurements of albumin egg as an eco-friendly inhibitor for copper corrosion in alkaline solutions

S. M. Syam, [iD] *[a] Ahmed. A. Elhenawy, [iD] [bc] Ehab Gad,[bd] H. Nady[de] and Salah Eid[ad]

Utilizing environmentally acceptable substances as inhibitors of metal corrosion is one of the most important strategies to reduce corrosion. In alkaline solutions (1.0 M KOH), the influence of albumin egg as a green corrosion inhibitor for copper was studied *via* a mix of experimental and theoretical investigations. Cyclic voltammetry (CV), open circuit potential (OCP), electrochemical impedance spectroscopy (EIS), potentiodynamic polarization (PDP), AFM, and SEM/EDX methods were all utilized to examine the inhibitory effect of albumin egg. By increasing the amount of albumin egg in the corrosive solution, the inhibition efficiency is increased. The albumin egg is a highly effective cathodic type inhibitor, according to electrochemical tests, with an inhibition efficiency of up to 94%. It also follows the Langmuir isotherm during adsorption. Investigations using SEM/EDX and AFM show that the albumin egg can create an adsorption layer on the surface enabling the shielding of the copper surface from harmful ions. In order to better understand the molecular structure of the albumin egg and its inhibitory action against corrosion, computational and molecular dynamics simulation techniques were also employed for calculating the electronic characteristics of inhibitor molecules. Calculations were made for total energy (TE), change in total energy (DET), energy gap (ΔE), E_{LUMO}, E_{HOMO}, dipole moment (D), and softness (δ). Utilizing the Monte Carlo simulation, the mechanism of albumin egg adsorption on the surface of Cu was investigated. The theoretical outcomes were found to confirm the empirical results.

1. Introduction

Copper is an adaptable and valuable material that has been extensively employed in electrical wiring, coinage, car industry, marine environment, water supply systems, oil refining and energetics due to its superior corrosion resistance, ductility, durability, and great thermal and electrical conductivity.[1,2] However, copper is susceptible to corrosion in both acidic and alkaline solutions, particularly in the existence of oxidants, such as chlorides and oxygen.[3] The use of corrosion inhibitors is the most popular technique that relieves or prevents the metallic substrate corrosion with the environment when added in a small amount. The inhibitor materials may be organic or inorganic chemicals. Many inorganic compounds, such as chromate, tetra borate, and molybdate, are utilized to minimize the copper corrosion rate.[4,5] Moreover, organic inhibitors are effective

because they adhere to the metal surface.[6–14] Their adsorption may be due to the presence of hetero atoms (O, N, and S), in addition to the conjugating aromatic rings.[15] The majority of inhibitors are poisonous, dangerous, and harmful to the nature, therefore, researchers try inexpensive, available, and renewable sources of green materials to preserve metals and alloys in diverse media.[16–19] Many naturally occurring compounds were studied and reported as good and effective corrosion inhibitors.[20–28] Egg albumin is one of the naturally occurring compounds that perform well as an anti-corrosion agent for some metals in diverse environments.[29–31] In this study, the effectiveness of egg albumin protein as an ecological inhibitor of copper corrosion in 1 M KOH was examined using OCP, PDP, CV, EIS, SEM/EDX, and AFM techniques. In addition, theoretical computation was used to support the experimental findings.

2. Experimental

2.1. Materials

Copper of 99.9% purity was enclosed in an epoxy resin mold leaving the small bottom region with a surface area of 0.12 cm^2 exposed to the aggressive environment. A copper electrode was mechanically abraded employing various emery sheet grades up to 2500 before every test, followed by rinsing with distilled water, acetone, and once again distilled water, and drying at

[a]Chemistry Department, Faculty of Science, Benha University, Benha, Egypt. E-mail: samar.seyam@fsc.bu.edu.eg

[b]Chemistry Department, Faculty of Science, Al-Azhar University, Nasr City, Egypt

[c]Chemistry Department, Faculty of Science Arts in Almakhwah, Albaha University, Abaha, Saudi Arabia

[d]Chemistry Department, College of Science and Arts, Jouf University, Alqurayat, Saudi Arabia

[e]Chemistry Department, Faculty of Science, Fayoum University, Fayoum, Egypt

room temperature. Potassium hydroxide as a corrosive medium and egg albumin as an eco-friendly inhibitor were purchased from Alpha Chemika. Stock solutions of KOH and egg albumin were prepared and then diluted to prepare appropriate concentrations.

2.2. Electrochemical measurements

Four techniques, namely, cyclic voltammetry (CV), open circuit potential (OCP), electrochemical impedance spectroscopy (EIS) and potentiodynamic polarization (PDP) techniques were applied utilizing Versa STAT 4 with the versa studio electrochemically software package. A platinum wire was employed as the counter electrode, a saturated calomel electrode (SCE) as the reference electrode, and copper as the working electrode in a three-electrode cell. The working electrode was submerged in the investigated solution prior to conducting any electrochemical studies and left for 15 min in an open circuit to allow open circuit potential (OCP) stabilization. The potentiodynamic polarization technique was displayed at 5 mV s^{-1}, and cyclic voltammetry at 100 mV s^{-1}. Measurements using EIS were made with an amplitude of 0.01 V over a frequency range of 100 000 Hz to 0.1 Hz.

2.3. Surface analysis

Various techniques were used to analyze the metal surface. Prior to each analysis, copper specimen was abraded, washed with distilled water, degreased with acetone and dipped in 1 M KOH for one day in the presence and absence of 4000 ppm albumin egg. After the period elapsed, the specimen were washed, dried and then kept in a desiccator till the surface analysis. For analyzing the surface morphology, a scanning electron microscope (SEM; BED-C 10.0KV, Jeol) equipped with an EDX unit was used. Atomic force microscopy (AFM) was carried out using a Nano Surf Flex AFM equipped with a C3000 controller.

2.4. Quantum chemical model

In order to conduct a theoretical examination, we employed the Materials Studio program (Accelrys Inc.[32]) and the computational density functional theory (DFT) with unlimited spin and the DMol3 module. We used the Becke3-Lee-Yang-parr (B$_3$LYP) level[33] with the double-numeric DNP basis set (DNP 4.4)[34] and the generalized gradient approximation (GGA). We looked at the electrical properties, LUMO and HOMO energies, and differences between them as well as other characteristics of albumin. We also followed the procedure reported by[33] to calculate chemical descriptors including nucleophilicity (ξ), electron affinity ($A = -E_{\text{LUMO}}$), ionization energy ($I = -E_{\text{HOMO}}$), back-donation energy ($\Delta E_{\text{back-donation}}$), chemical hardness ($\eta$), transported electrons (ΔN) from LUMO and HOMO energies, electronegativity (μ), chemical softness (σ), electroaccepting power ($\omega+$), electrodonating power ($\omega-$), and electrophilicity (ω) of albumin.[33]

2.5. Molecular dynamics simulations

Molecular dynamics (MD) simulation was utilized to investigate the adsorption of albumin inhibitors onto the copper surface in

alkaline media. We chose the Cu (110) plane as the most stable surface for the simulation. We created a simulation box (22.90 Å × 57.26 Å × 26.68 Å) with a Cu slab and a vacuum layer of 15.00 Å. We calculated the adsorption energy of inhibitors on the Cu surface using eqn (1):

$$E_{\text{adsorption}} = E_{\text{total}} - (E_{\text{Cu}} + E_{\text{inhibitor}}) \qquad (1)$$

where E_{total} is the system total energy, E_{Cu} the Cu slab energy, and $E_{\text{inhibitor}}$ the energy of inhibitor molecule. The binding energy was computed as the adsorption energy's negative value. The interatomic interaction between the Cu metal and albumin can be verified by the density of state (DOS) analysis. The DOS analysis was performed using the CASTEP in the MS packages,[32] which uses the Perdew–Burke–Ernzerhof (PBE) functional for the exchange-correlation energy and the generalized gradient approximation (GGA) for the gradient.

3. Results and discussion

3.1. OCP measurements

The open-circuit potential of the copper electrode as a parameter depends on the immersion time. The OCP for the copper electrode in KOH (1.0) solutions without and with different amounts of albumin egg was measured, and is presented in Fig. 1. The curves demonstrate that the existence of albumin egg causes the steady-state potential to change to a greater negative value. This might be explained by the albumin egg molecules sticking to the active regions of the copper surface. It also appears that as the albumin egg concentration increases, the OCP shifts further to a negative value, which means that the cathodic reaction was predominant.[35–37]

3.2. Cyclic voltammetry

Cyclic voltammetry plots for copper in 1 M KOH devoid of and containing diverse amounts of albumin egg are shown in Fig. 2. One cathodic and three anodic peaks may be observed in the
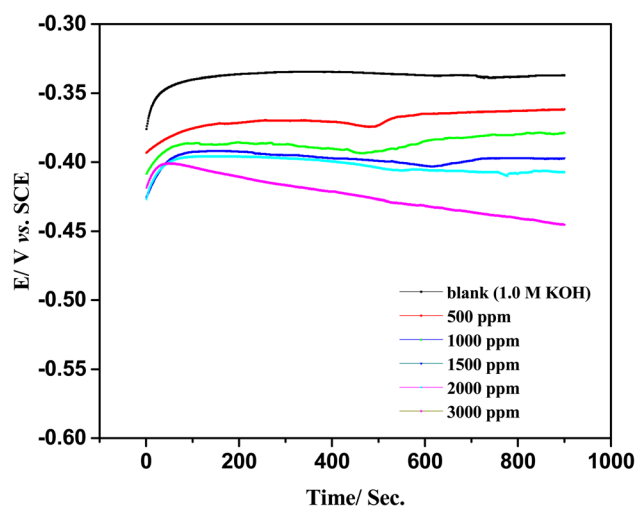

Fig. 1 OCP of Cu in 1.0 M KOH solutions containing different concentrations of albumin egg.
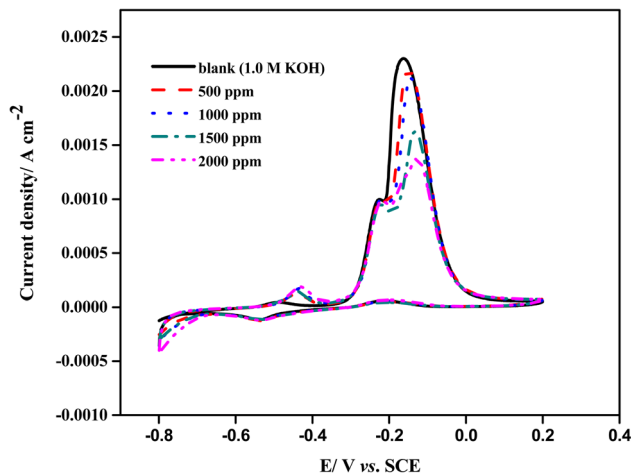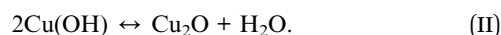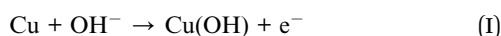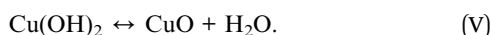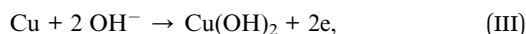
Fig. 2 CV curves for the Cu electrode in 1.0 M KOH solutions containing different concentrations of albumin egg.

cyclic voltammetric curves.[38-42] The first peak may be correlated with the electroformation of the Cu_2O mono layer.

$$Cu + OH^- \rightarrow Cu(OH) + e^- \qquad (I)$$

$$2Cu(OH) \leftrightarrow Cu_2O + H_2O. \qquad (II)$$

The second and third peaks may be correlated with the CuO multilayer anode formation.

$$Cu + 2 OH^- \rightarrow Cu(OH)_2 + 2e, \qquad (III)$$

$$Cu(OH) + OH^- \leftrightarrow Cu(OH)_2 + e^- \qquad (IV)$$

$$Cu(OH)_2 \leftrightarrow CuO + H_2O. \qquad (V)$$

The reduction peak may be correlated with the electro-reduction of CuO to Cu_2O and Cu_2O to Cu.

$$2CuO + 2e^- + H_2O \rightarrow Cu_2O + 2OH^-, \qquad (VI)$$

$$Cu_2O + 2e^- + H_2O \rightarrow 2Cu + 2OH^-. \qquad (VII)$$
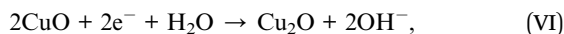
The rate of oxide film formation decreased as the albumin egg concentration increased. This caused a reduction in anodic and cathodic peaks and, hence, reduced the charge of oxidation–reduction reactions.[38-42]

3.3. Potentiodynamic polarization

Fig. 3a represents the polarization plots of Cu in KOH (1.0 M) devoid of and containing various amounts of albumin egg at a scan rate of 5×10^{-3} V s^{-1}. The relevant electrochemical data such as the corrosion potential, E_{corr}, corrosion current density, i_{corr}, inhibition efficiency, %IE, and cathodic anodic Tafel slopes (β_c and β_a) were calculated from the extrapolation method, and are recorded in Table 1. The inhibitory efficiency and surface coverage values were obtained from the subsequent eqn (2) and (3):

$$\%IE = \frac{i_{corr}^\circ - i_{corr}}{i_{corr}^\circ} \times 100 \qquad (2)$$

$$\Theta = \frac{i_{corr}^\circ - i_{corr}}{i_{corr}^\circ} \qquad (3)$$

where i_{corr}° and i_{corr} are the corrosion current densities devoid of and containing various concentrations of albumin egg, respectively. It can be observed from Fig. 3a that as albumin egg was added at various concentrations to potassium hydroxide solutions, the curves shifted to lower current densities, which, in turn, caused a decrease in the rate of corrosion and an increase in the inhibition efficiency. From Table 1 and Fig. 3b, the inhibition efficiency enhanced as the albumin egg concentration increased. The value of %IE reached its maximum, 94%, at 4000 ppm. Even at a lower amount of 500 ppm, the inhibition efficiency was 62%. This increase in inhibition efficiency may be due to two factors: first, the increasing amount of adsorbed molecules on the copper surface and, second, the large size of albumin egg molecules, of which a small number of molecules need to be adsorbed to cover the entire copper surface.[43,44] In addition, when the concentration of the inhibitor increased, the
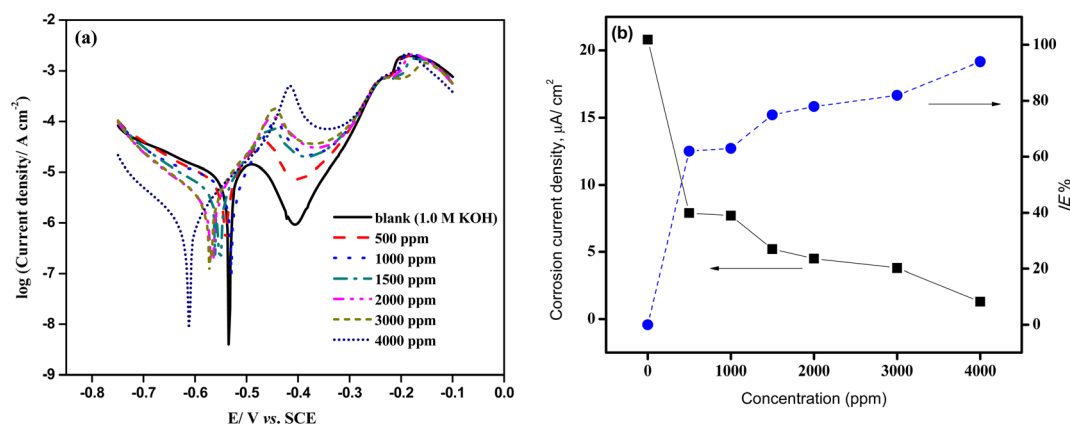

Fig. 3 Potentiodynamic polarization curves of Cu after electrode immersion in stagnant 1.0 M KOH without and with various concentrations of albumin egg.

Table 1 Polarization parameters of copper in the absence and presence of different concentrations of inhibitors in aerated stagnant 1.0 M KOH

Inh. Conc.	E_{corr} (mV$_{(SCE)}$)	i_{corr} (µA cm^{-2})	β_a (mV dec^{-1})	β_c (mV dec^{-1})	Θ	$\eta\%$
0	−530.1	20.8	145.1	362.0		
500	−542.7	7.9	87.4	255.6	0.620	62
1000	−529.6	7.7	87.2	378.7	0.63	63
1500	−558.5	5.2	95.0	208.6	0.75	75
2000	−554.4	4.5	82.3	195.0	0.78	78
3000	−57.4	3.8	95.3	160.0	0.82	82
4000	−615.1	1.3	106.2	142.8	0.94	94

values of E_{corr} slightly shifted towards negativity, while the cathodic Tafel constant values changed by more than 85 mV, indicating that the albumin egg works as a cathodic inhibitor.[45,46]

To understand the relation between the molecular structure of corrosion inhibitors and their inhibition efficiency, a comparison between the experimental results of this work and those of previous works on copper corrosion inhibitors in diverse environments is shown in Table 2. According to PDP measurements, the albumin egg acts as a good corrosion inhibitor for copper in alkaline media.

3.4. EIS measurements

With its ability to explore the relaxation phenomena with relaxation times that range across orders of magnitudes and the ability to perform single averaging within a single experiment to achieve extremely accurate levels, EIS is a steady-state approach. This validates the polarization methods for measuring the corrosion rate. The Cu electrode was used for EIS studies in 1 M KOH alone and in combination with different amounts of albumin egg present at OCP. Similar characteristics to several semicircles, which are the depressed capacitive loops, can be seen in the impedance spectra. It is noteworthy to note that each semicircle's diameter increases sharply with the increase in the concentration of albumin egg, referring to the formation of a protective adsorbed layer, which enhances the corrosion resistance.[47] In Fig. 4, the effects of increasing albumin egg concentration on Cu electrode impedance plots are demonstrated using a Bode plot, which depicts the relationship between impedance magnitude, $|Z|$, phase angle, and log

frequency. The EIS spectra indicate that the equivalent circuit of the system must have numerous time constants and that mass movement *via* the phase layer should be taken into account. There are two phase maxima at the low and middle frequencies of every Bode spectrum. The existence of a second-phase maximum at low frequencies and the lack of an impedance plateau indicate the presence of a diffusion process.[47] As displayed in Fig. 4, the phase angles of the copper electrode in a KOH solution containing albumin egg are obviously greater than those in aggressive media in both the high- and low-frequency ranges. The electrode's frequency range is noticeably greater in albumin egg-containing liquids, suggesting that the preservative layer may retain its distinctive response for a longer period of time. The size of semi-circle in the Nyquist plot expands with the increasing albumin egg concentration, as shown in Fig. 4. This implies an increase in the impedance value, suggesting that albumin egg molecules hinder the dissolution of the Cu electrode, which is consistent with the polarization investigations results. The software of impedance equipment and the dispersion formula were used to examine the impedance values. For a simple equivalent circuit model that consists of a parallel connection of a capacitance, C_{dl}, and a resistor, R_{ct}, in series with a resistor, R_s, that exemplify the resistance of solution, the electrode impedance, Z, was exemplified using mathematical formulation (4).

$$Z = R_s + \frac{R_{ct}}{1 + (2\pi f R_{ct} C_{dl})^\alpha} \quad (4)$$

where α gives an empirical parameter ($0 \leq \alpha \leq 1$) and f refers to the frequency in Hz. The dispersion formula takes into

Table 2 Comparison of the inhibition efficiencies of different Cu inhibitors in different environments

| Inhibitor	Concentration	Metal	Medium	Inhibition efficiency	Ref.
Creatine	500 mg L^{-1}	Cu	0.5 M NaOH	89.7%	20
Creatinine				86.4%	
Caffeine	10 mmol L^{-1}	Cu	0.1mmol L^{-1} H$_2$SO$_4$	72.0%	21
Oleuropein	100 mg L^{-1}	Cu	1 M H$_2$SO$_4$	97.0%	26
Citrullus colocynthis fruits	0.075 g L^{-1}	Cu	1 M H$_2$SO$_4$	90.6%	27
			1 M NaOH	84.6%	
			1 M NaCl	77.1%	
Alchemilla vulgaris (ALV) extract	7 g L^{-1}	Cu	1 M HCl	96.0%	28
Cysteine	16 mM	Cu	0.6 M NaCl	76.6%	36
	18 mM		1 M HCl	84.1%	
Albumin egg	4000 ppm	Cu	1 M KOH	94.0%	This work
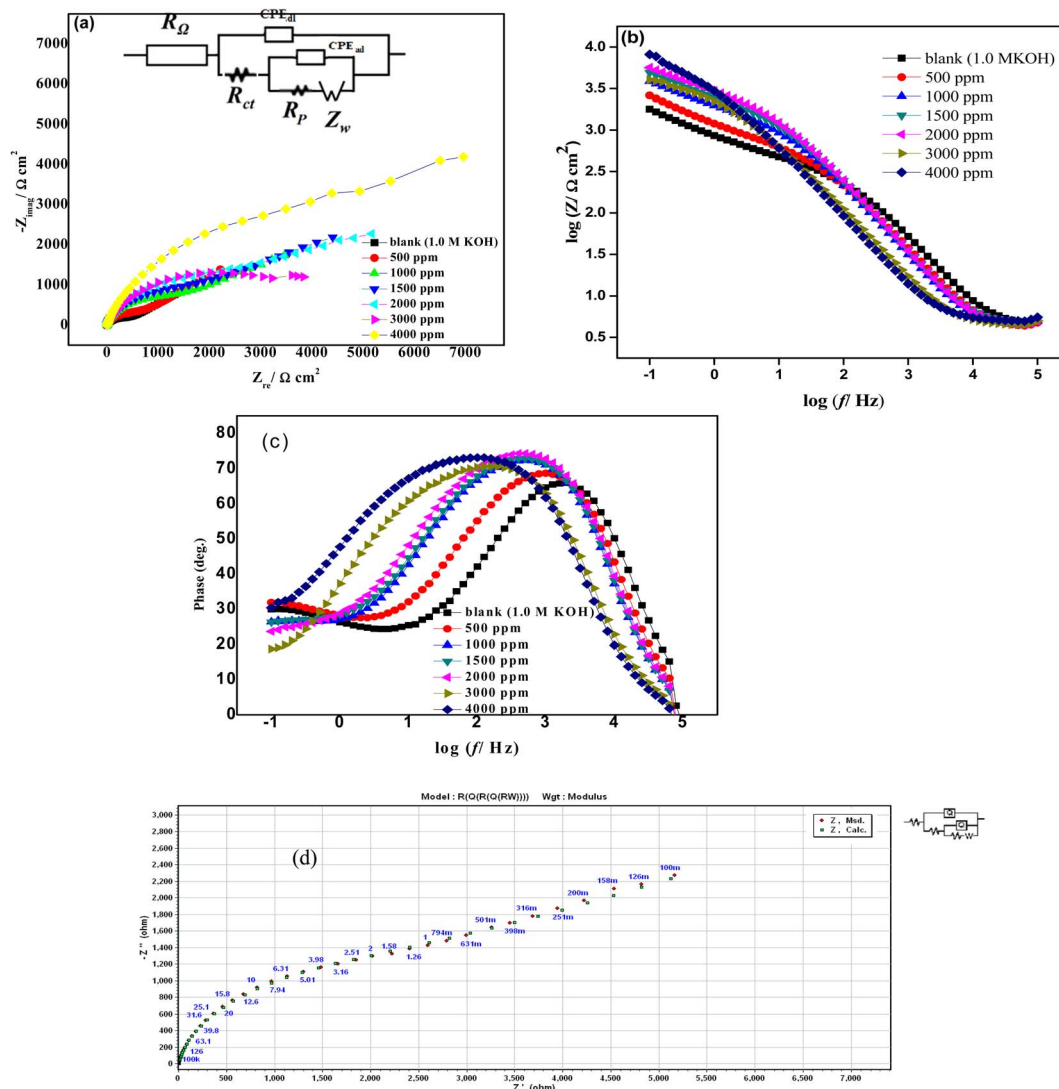
Fig. 4   EIS curves of Cu in alkaline solutions containing different concentrations of albumin egg.

consideration departures from the ideal RC-behavior in terms of the distribution of time constants caused by surface roughness, heterogeneity, and diversity in either features of surface coating or the compositions.[48,49]

Besides the corroding interface at a lower frequency, an adsorbed albumin egg layer was formed at the intermediate frequency, where different Rpf Cpf combinations were created to explain the spontaneity of the passive film formation. The impedance data for the copper electrode might be precisely comprehended using the analogous circuit depicted in Fig. 4. The characteristics of the appreciated equivalent circuit for the copper electrode at various albumin egg doses are displayed in Table 3. The findings in Table 3 shed light on the way in which the adsorbed coating is being developed on the copper surface, its protective properties, and how it improved the corrosion resistance of Cu electrodes. The EIS findings are in agreement with the potentiodynamic polarization data reported earlier.

3.5.   Adsorption isotherm

It is commonly accepted that the adsorption isotherm is a helpful tool for shedding light on the inhibitory process's mechanism. The surface coverage values, θ, for albumin egg adsorption on the Cu surface were determined using PDP measurements. Various adsorption isotherms were tested on the preliminary results from PDP measurements to determine the best isotherm.[50] To comprehend the process at work in the case of albumin egg (Fig. 5), the Frumkin, Freundlich, Al Awady, Temkin, Flory-Huggins, and Langmuir isotherms[50] were investigated. Our findings meet the Langmuir isotherm formula (5):[51]

$$\frac{C}{\theta} = \frac{1}{K} + C \qquad (5)$$

where C is the concentration of albumin egg and K is the adsorption equilibrium constant. The graph of $\frac{C}{\theta}$ *versus* C is shown in Fig. 5, which results in straight lines with slopes equal

Table 3 Electrochemical parameters calculated from the EIS measurements on the copper electrode in 1.0 M KOH solutions without and with various concentrations of inhibitors at 25 ± 1 °C

Conc. ppm	R_s (Ω cm^2)	R_1 (Ω cm^2)	Q_1Y_o (Ω^{-1} cm^{-2} s^{n2})	R_{ad} (Ω cm^2)	Q_2Y_o (Ω^{-1} cm^{-2} s^{n2})	$R_p = R_1 + R_{ad}$ (Ω cm^2)	W (Ω^{-1} cm^{-2} s$^{0.5}$)	$\eta\%$
0	9.6	135.6	5.055×10^{-6}	746	54.54×10^{-5}	881.6	—	—
500	4.2	0.2	6.9×10^{-5}	921.7	3.0×10^{-6}	921.9	0.0005506	4.371407
1000	4.5	14.56	4.07×10^{-6}	1934	4.39×10^{-5}	1948.56	0.000463	54.75633
3000	4.9	45.14	4.6×10^{-6}	4812	2.98×10^{-5}	4857.14	0.00166	81.8494
4000	4.8	14.97	9.08×10^{-5}	6452	5.16×10^{-5}	6466.97	0.00030	86.36765

to unity and a $[1/K]$ intercept. The connection of the standard adsorption free energy, ΔG°_{ads}, with K is described according to the following formula (6):[24].

$$ k = \frac{1}{1000} \exp \frac{\Delta G^{\circ}_{ads}}{RT} \tag{6} $$

where 1000 g L^{-1} refers to the H$_2$O concentration, T indicates the absolute temperature, and R is the gas constant. ΔG°_{ads} for adsorbed albumin egg on the surface of copper in KOH (1.0 M)

is -18.789 kJ mol^{-1}, while K is 1.9657. Albumin egg spontaneously adsorbs onto the copper surface, as proved by the negative value of ΔG°_{ads}.[52] The obtained significantly small ΔG°_{ads} value suggests that the nature of adsorption of albumin egg onto the copper surface is physical.[24]

3.6. SEM, EDX and AFM investigations

It was possible to determine how sharp the corrosion attack was by examining the surface's shape. Copper coupons were
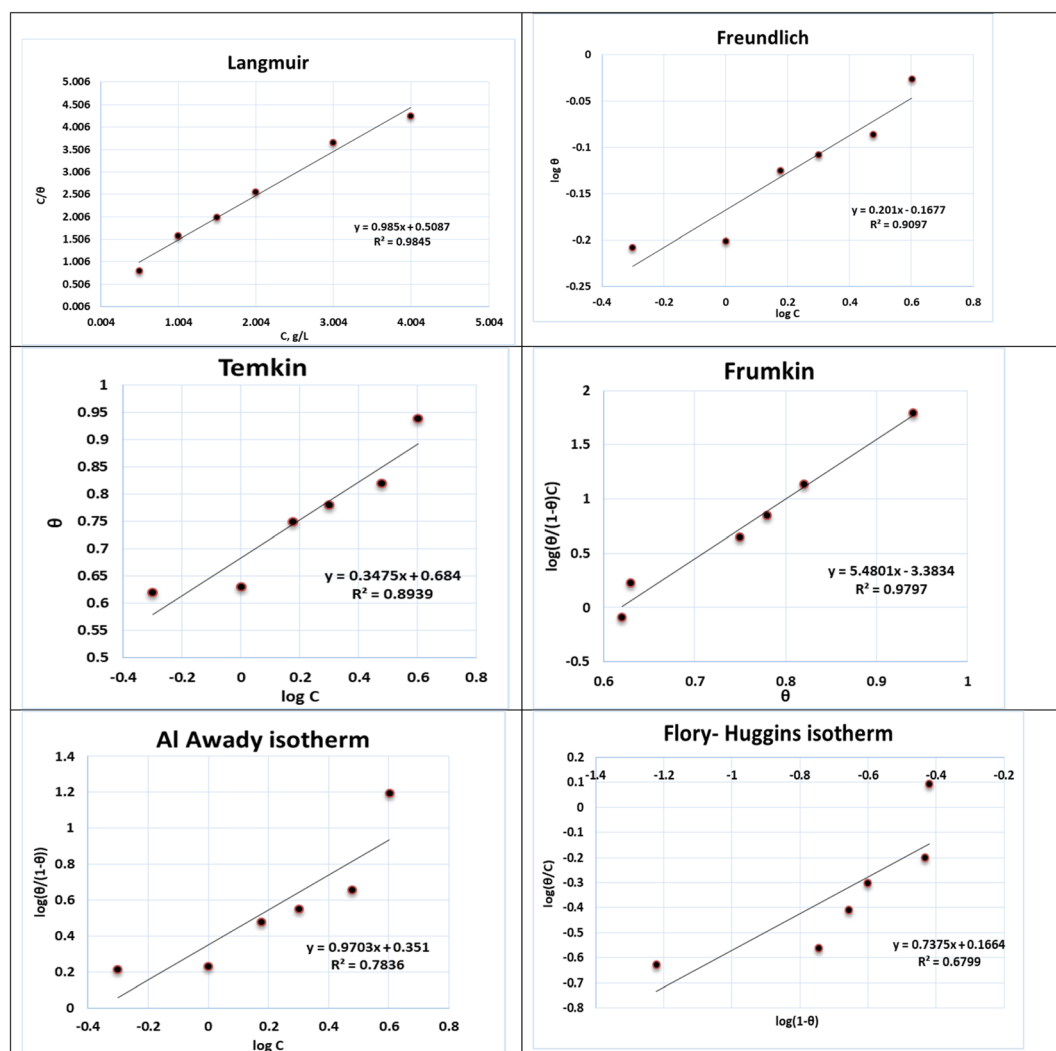

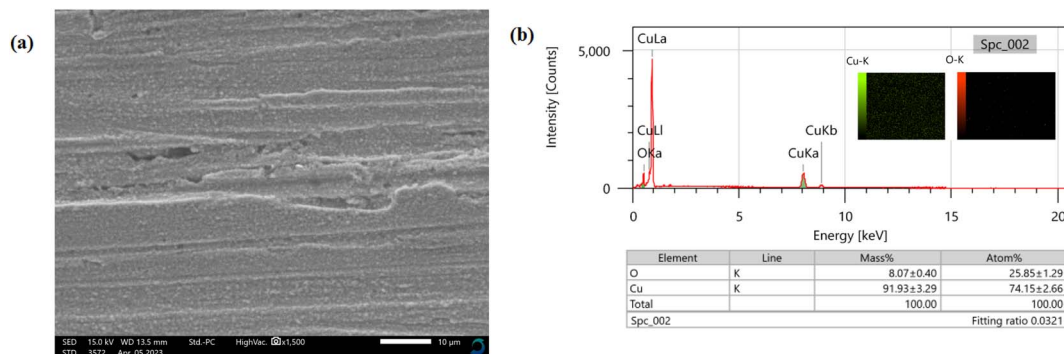**Fig. 5** Adsorption isotherms of albumin egg on Cu electrodes in 1.0 M KOH.

Fig. 6 SEM image/EDX pattern of the Cu surface after electrode immersion in a 1.0 M KOH solution.
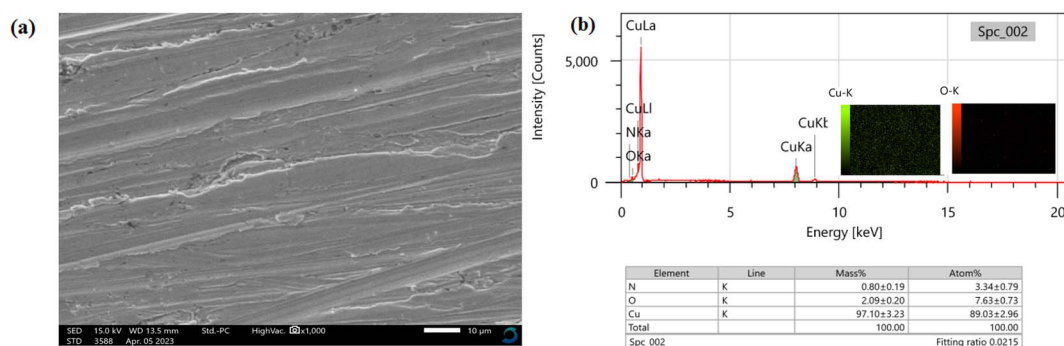

Fig. 7 SEM image/EDX pattern of the Cu surface after electrode immersion in a 1.0 M KOH solution containing 4000 ppm of the investigated inhibitor.

observed by SEM after dipping in 1.0 M KOH lacking and possessing 4000 ppm of albumin egg, as shown in Fig. 6 and 7. Copper coupons in 1.0 M KOH only showed a significantly distorted surface according to the SEM data, which described their morphology. Otherwise, the copper surface gets smoother and less deteriorated in a 1 M KOH solution with albumin egg.[53–55]

The surface roughness of a coupon can be assessed with the surface topography images acquired using an AFM. The AFM morphologies for the copper surface in 1.0 KOH solutions are shown in Fig. 8 and 9 for both the albumin egg-free and albumin egg-containing solutions. According to Fig. 8 and 9, the values of average roughness and root mean square for the copper surface in 1 M KOH are higher than those for an copper
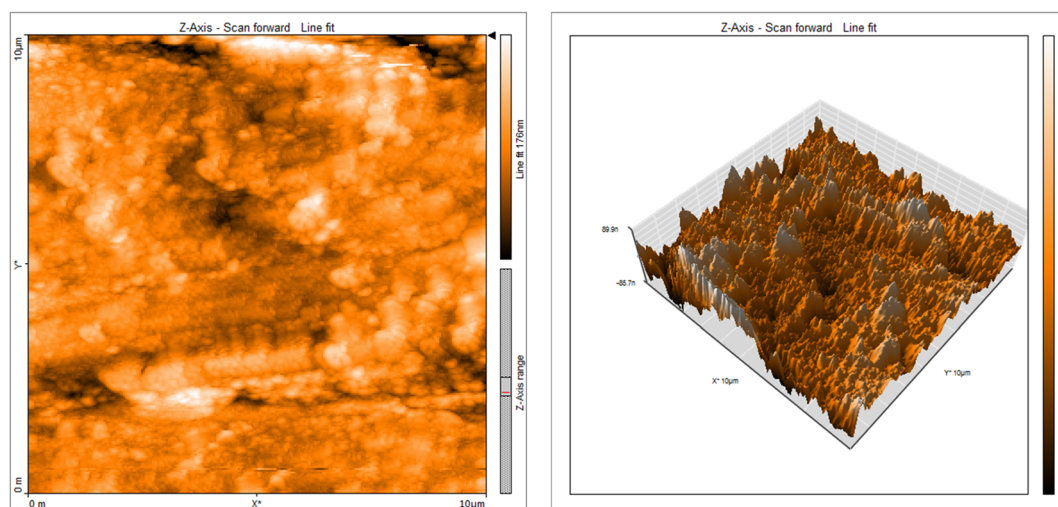

Fig. 8 AFM image of the Cu surface after electrode immersion in a 1.0 M KOH solution.
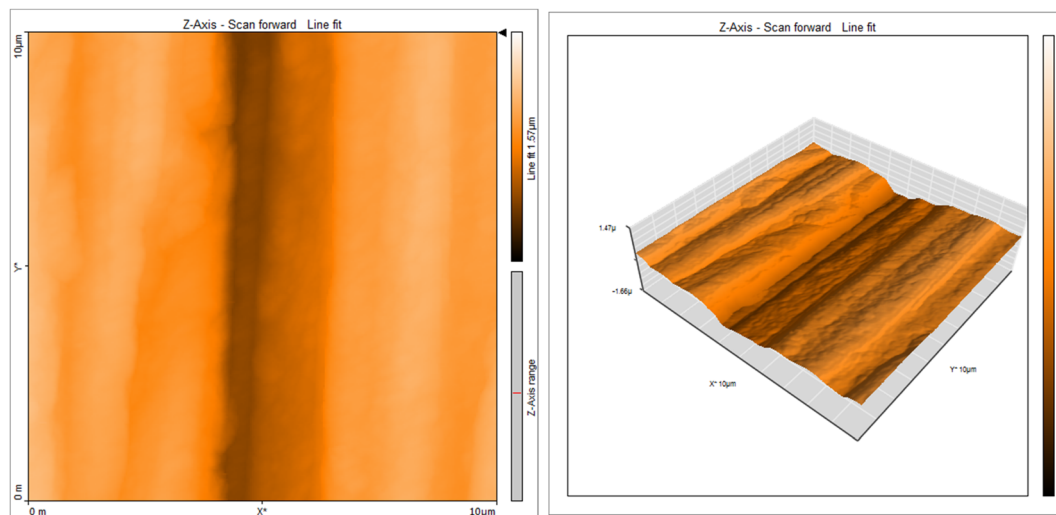
Fig. 9 AFM image of the Cu surface after electrode immersion in a 1.0 M KOH solution containing 4000 ppm of the investigated inhibitor.

sample in the presence of albumin egg, which are 209.16, 304.66 nm and 163.10, 209.10 nm, respectively.[56] These findings demonstrate the adsorption of albumin egg onto the copper surface, where they have successfully created a shielding layer that protects the surface of copper from harmful ions.[56,57]

3.7. Albumin frontier molecular orbital "FMO" profile

We used density functional theory (DFT) at the B3LYP/6-311 level to optimize the geometry with unconstrained spin to provide the best comprehension of the molecular structure of albumin as a corrosion inhibitor, as illustrated in Fig. 10.

The most important orbitals for albumin molecules are the lowest unoccupied molecular orbital (LUMO), which accepts electrons, and the highest occupied molecular orbital (HOMO), which donates electrons. These orbitals are called the FMO, and they determine the interaction pathway with the Cu surface. We used the simple Hückel Molecular Orbital Theory (SHMO)[58] to calculate the FMO gap, which indicates the chemical reactivity and molecule kinetic stability. A strong interaction is formed between the albumin egg inhibitor with a higher HOMO energy and the copper surface with a lower LUMO energy.[59] The main function of an albumin inhibitor is the bond formation between the surface of copper and its d-orbital electrons, by donating and accepting electrons. The S0 state shows the E_{HOMO} and E_{LUMO} values of an albumin inhibitor. As shown in Table 4, albumin has a high E_{HOMO} value, which means that it can easily
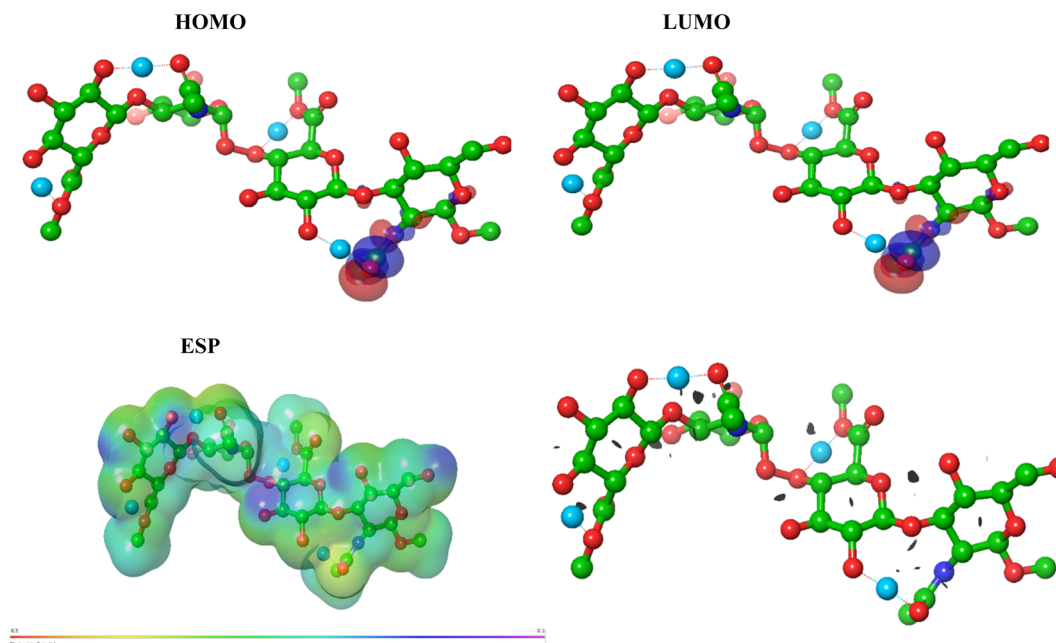

Fig. 10 Plotted FMOs and ESP for tested compounds.

Table 4 Calculated charge, energetic and reactivity parameters for albumin inhibitors

HOMO	−5.988
LUMO	−0.716
ΔG	5.273
Hard	2.636
Soft	0.379
Electronegativity	−3.352
EP	3.352
Electrophilcty	2.131
$U+$	−2.034
$U-$	−4.670
TNC	−0.26
I	5.988
A	84.365
$W-$	84.365
$W+$	1.801
$w+-$	−12.312
ΔE_{max}	1.271
$\Delta E_{Back\text{-}donation}$	−0.659
ΔN_{max}	−0.636
$W+$	1.801
$w-$	4.136

give up electrons to the Cu surface and enhance albumin inhibitory effects.[59,60] The HOMO and LUMO orbitals are concentrated on the C=O group of the acetamide moiety (Fig. 10). The negative values of E_{HOMO} and E_{LUMO} elucidate that there is a transfer of charge from the albumin egg molecules to the copper surface. This suggests that the C=O group is the effective site for the albumin molecule adsorption on the copper surface.

3.8. Molecular electrostatic potential (ESP)

To put ESP more simply, the way in which molecules push and pull on each other with electric forces (ESP) can change how the albumin inhibitor stops a copper surface from reacting.[61] The ESP has two kinds of forces: pushing forces (blue) and pulling forces (yellow and red) that come from the atoms and electrons in an albumin molecule. Fig. 10 shows the ESP for an albumin inhibitor, which has negative charges on its C=O and OH parts. The different color combinations on the ESP surface show the different electric forces. A bigger positive area on the albumin inhibitor means that it can go deeper into the copper surface, making it more effective at stopping reactions.

3.9. Global chemical reactivity

This work presents a study on the binding interaction between the HOMO of albumin egg and the LUMO of a Cu-surface, which shows how well a compound can adsorb onto the surface of metals. The efficiency of adsorption of a compound onto the surface of metals was determined by the stability index, which was measured by the energy gap (ΔG). In addition, we studied the correlation between soft and hard nucleophiles/electrophiles and the ΔG values, where molecules with a low softness feature are expected to be efficient corrosion inhibitors, while hard molecules are expected to be inefficient

corrosion inhibitors.[62] As can be observed from Table 4, the albumin compound has a great softness value, thus our results indicate that albumin has a high inhibition efficiency against the copper surface with a ΔG value of 5.2 eV (Table 4). One of the aspects that affects the inhibition of copper corrosion by albumin inhibitors is the interaction between the negative cores of the albumin egg and the copper surface. The total negative charge (TNC) of the albumin inhibitor reflects its ability to penetrate and adsorb onto the copper surface, thus reducing the corrosion rate.[63] Moreover, the electron donating potency ($\mu-$) and capacity ($\omega-$) of the inhibitor indicate its tendency to transfer electrons from itself as a donor to the metal as an acceptor.[63] These parameters are related to the inhibition potency of the albumin inhibitor for copper corrosion.

The albumin inhibitor interacts with the surface of the Cu metal by accepting or donating electrons, which affects the inhibitory activity. The cumulative electrons donating for albumin inhibitor ($\mu- = 4.6$ eV and $\omega- = 8.3$ eV), the higher the inhibition efficiency, as it reduces the metal oxidation. The opposite is true for electron accepting ($\mu+$ and $\omega+$), which enhances the corrosion of the Cu metal. The maximum number of electrons transferred (ΔN_{max}) and energy back donation term ($\Delta E_{Back\text{-}donation}$) are important factors that govern the bond strength among copper and albumin egg, which can be calculated using DFT/B3LYP.

It can be inferred that the albumin molecule has high inhibition efficiency. The elevated value of $\Delta E_{Back\text{-}donation}$ suggests that the albumin egg can penetrate powerfully into the surface of the Cu metal. Moreover, the negative values of $\mu+$ and $\omega+$ demonstrate that the electron transfer from the Cu metal to albumin egg is energetically favored, which further supports the inhibitory effect of the molecule.

3.10. Molecular dynamics simulation and mechanism of inhibition

Molecular dynamics (MD) simulation was used to inspect the movement and attitude of atoms and molecules over time; in the context of inhibitor-Cu surface interactions, MD simulations can help provide a more detailed understanding of the underlying mechanisms. An optimization geometry was performed for albumin before running the adsorption process, which probably refers to the inhibitor molecule. This step is important to ensure that the molecule is in an energetically favorable geometry prior to adsorption. The perfect and favorable site of adsorption for the copper surface against albumin egg molecules can be identified by an adsorption locator model (Fig. 11), which has the following lowest calculated energies expressed in kcal mol^{-1}, as listed in Table 5; total energy (substrate-adsorbate energy), rigid adsorption energy (rigid albumin component adsorbed onto the Cu-metal surface), deformation energy (deformed albumin components adsorbed onto the metal surface), adsorption energy: (rigid adsorption and deformation energies), dEads/dNi (metal-inhibitor energy with one inhibitor molecule removed; the change in adsorption energy per molecule when one albumin molecule has been removed from the system), interaction energy (the strength of

interaction between the albumin egg and the copper surface), and electrostatic energy.

There is energy contribution from electrostatic interactions between charged species in the system. The key findings are as follows:

- Albumin acts as a corrosion inhibitor for Cu-surface *via* formation of a stable complex with copper atoms.

- Albumin binds to copper through its hydrophobic parts.

- Albumin adopts a coplanar conformation that is analogous to the Cu (110) surface plane, as manifested in Fig. 10.

- The negative adsorption energy value manifests that the albumin adsorption is more favorable in alkaline media (Table 5).

The key mechanism seems to be the formation of a stable albumin–copper complex *via* hydrophobic interactions, and the coplanar adsorption of this complex onto the aluminum surface. The theoretical observation is in line with our experimental finding. Based on the information provided, it is possible to make the inference that albumin inhibitors can act as efficient corrosion inhibitors for Cu in alkaline solutions. Fig. 10 may exhibit the evidence of the albumin inhibitor's adsorption onto the surface of Cu through the hydrophilic part of the inhibitor, which may create a preservative layer on the metal surface (Fig. 12). This layer could potentially prevent Cu from interacting with an alkaline solution, thus reducing the rate of corrosion.

Table 5 Binding energy expressed in kcal mol^{-1} for albumin against the Cu surface

Total energy	71.059
Adsorption energy	−567.672
Rigid adsorption energy	−16.356
Deformation energy	−551.316
dEad/dNi	−567.672

3.11. Density of states

In order to best understand the electrical interactions between the Cu (110) surface and the albumin inhibitor, the density of states (DOS) of the surface atoms in the more stable complex configuration was assessed. By comparing the difference between the DOS curves after and before the adsorption phenomena, the type of electron transfer that occurs during the method under study can be inferred. Fig. 13 presents the results that were found. The DOS curves show that the Cu (110) surface has strong hybridization with the albumin inhibitor, which indicates a chemisorption process. The Cu d-band shifts towards lower energies after adsorption, suggesting a charge transfer from the surface of the Cu metal to the inhibitor. This charge transfer enhances the stability of the Cu–Albumin complex and reduces the oxidation tendency of the Cu surface. The albumin inhibitor also forms a self-limiting monolayer on the Cu (110) surface, which acts as a physical barrier against
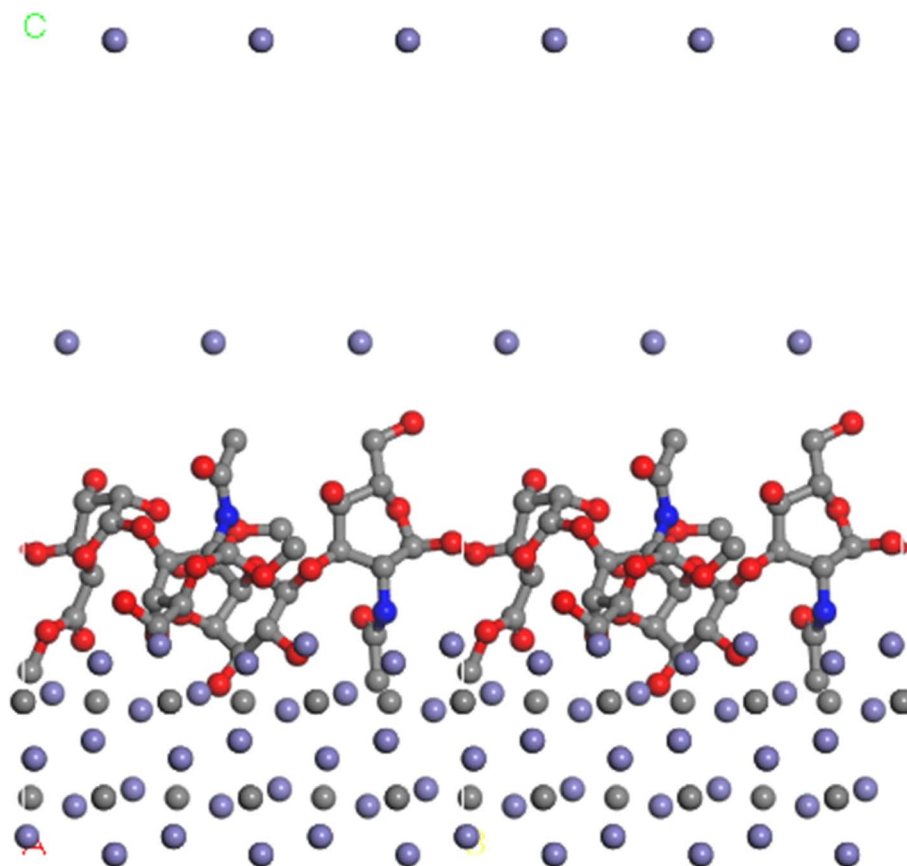

Fig. 11 Molecular dynamics simulations of the most favorable modes of adsorption for albumin inhibitors on the Cu (110) surface.
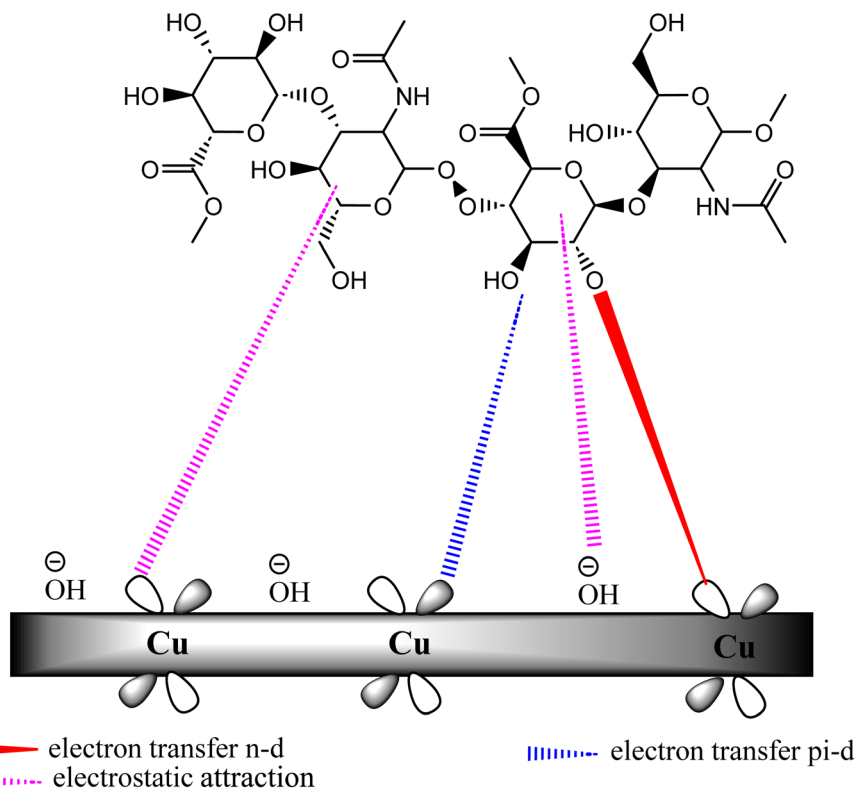
Fig. 12 Mechanism of adsorption of albumin egg onto the copper surface.
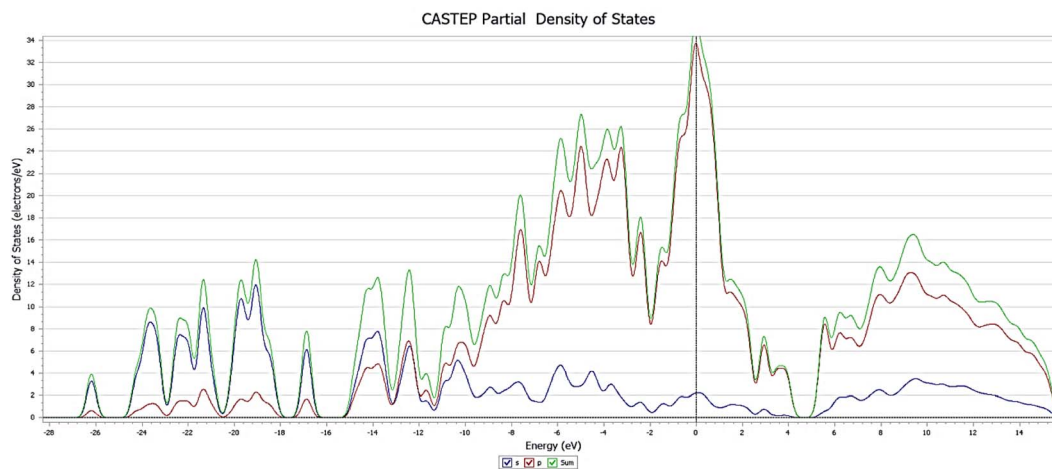

Fig. 13 DOS plot showing the Fermi orbitals for s and d orbitals.

corrosive agents. The Fermi level is represented by a straight line that is dotted at zero energy. The DOS peaks of isolated d fundamentally comprise d orbitals. When adsorption occurs, these orbitals of Cu shift to the left, indicating a lower energy level. Moreover, the offset peaks have a higher intensity than that of the isolated Cu surface (before adsorption). The interaction mechanism between the orbits involved in the adsorption process was confirmed by the decrease in the total energy of the complex. The Cu peaks near the Fermi level became more pronounced after the adsorption of the inhibitor, suggesting strong chemisorption between the Cu (110) surface and the albumin atoms. The electronic structure of all complexes changed significantly above the Fermi energy due to adsorption.

4. Conclusions

● Copper corrosion in 1.0 M KOH is diminished by adding albumin egg, and the level of inhibition depends on the albumin egg concentration.

● Albumin egg adsorption onto copper surfaces follows the Langmuir isotherm in KOH solutions.

● Albumin egg adsorption onto the surface of copper, which acts as a charge and mass transfer barrier to shield the copper surface from harmful ions in KOH solutions, is the basis for the inhibitory action.

● Reactivity indices, FMO, and MEP map investigations were carried out to look into potential albumin interaction centers with the Cu surface. The ability to gather very useful qualitative and quantitative data for determining the capacity of adsorption of albumin onto graphite and to better understand the mechanisms of adsorption of these metals is made possible by DFT and molecular dynamics simulation analysis.

● Based on the results and connections with quantum chemical and molecular dynamics characteristics, a more thorough explanation of how albumin is adsorbed onto the copper metal surface is provided.

Institutional review board statement

All procedures were performed in accordance with the Guidelines for Care and Use of Laboratory of Benha University and approved by the Ethics Committee of faculty of science (No. 39).

Author contributions

S. M. Syam performed conceptualization, investigation, methodology, resources, formal analysis, data curation, writing-original draft and writing-review and editing. Ahmed. A. Elhenawy did conceptualization, investigation, methodology, resources, formal analysis, data curation, writing-original draft and writing-review and editing. Ehab Gad did conceptualization, investigation, methodology, resources, formal analysis, data curation, writing-original draft and writing-review and editing. H. Nady gave conceptualization, investigation, methodology, resources, formal analysis, data curation, writing-original draft and writing-review and editing. Salah Eid performed conceptualization, investigation, methodology, resources, formal analysis, data curation, writing-original draft and writing-review and editing.

Conflicts of interest

The authors declare no conflict of interest.

References

1 P. Niamien, et al., Copper corrosion inhibition in 1 M HNO3 by two benzimidazole derivatives, Int. Scholarly Res. Not., 2012.

2 M. Sobhi and S. Eid, Chemical, electrochemical and morphology studies on methyl hydroxyethyl cellulose as green inhibitor for corrosion of copper in hydrochloric acid solutions, Prot. Met. Phys. Chem. Surf., 2018, 54, 893–898.

3 D. K. Verma, et al., Gravimetric, electrochemical surface and density functional theory study of acetohydroxamic and benzohydroxamic acids as corrosion inhibitors for copper in 1 M HCl, Results Phys., 2019, 13, 102194.

4 M. Vukasovich and J. Farr, Molybdate in corrosion inhibition—A review, Polyhedron, 1986, 5(1–2), 551–559.

5 A. Fateh, M. Aliofkhazraei and A. Rezvanian, Review of corrosive environments for copper and its corrosion inhibitors, Arabian J. Chem., 2020, 13(1), 481–544.

6 G. Tansuǧ, et al., A new corrosion inhibitor for copper protection, Corros. Sci., 2014, 84, 21–29.

7 T. Ma, et al., Corrosion control of copper wiring by barrier CMP slurry containing azole inhibitor: combination of simulation and experiment, Colloids Surf., A, 2020, 599, 124872.

8 K. W. Shinato, A. A. Zewde and Y. Jin, Corrosion protection of copper and copper alloys in different corrosive medium using environmentally friendly corrosion inhibitors, Corros. Rev., 2020, 38(2), 101–109.

9 I. H. Omar, F. Zucchi and G. Trabanelli, Schiff bases as corrosion inhibitors of copper and its alloys in acid media, Surf. Coat. Technol., 1986, 29(2), 141–151.

10 I. O. Althobaiti, et al., Evaluation of the Impact of Two Thiadiazole Derivatives on the Dissolution Behavior of Mild Steel in Acidic Environments, Molecules, 2023, 28(9), 3872.

11 S. Issaadi, T. Douadi and S. Chafaa, Adsorption and inhibitive properties of a new heterocyclic furan Schiff base on corrosion of copper in HCl 1 M: experimental and theoretical investigation, Appl. Surf. Sci., 2014, 316, 582–589.

12 M. Behpour, et al., Evaluating two new synthesized S–N Schiff bases on the corrosion of copper in 15% hydrochloric acid, Mater. Chem. Phys., 2008, 107(1), 153–157.

13 M. Antonijevic and M. Petrovic, Copper corrosion inhibitors. A review, Int. J. Electrochem. Sci., 2008, 3(1), 1–28.

14 S. Eid, S. M. Syam, A. Y. El-Etre and N. H. El Sayed, Surface, electrochemical, and theoretical investigation on utilizing olive leaf extract as green inhibitor for copper corrosion in alkaline environment, Arabian J. Sci. Eng., 2023, DOI: 10.1007/s13369-023-07940-4.

15 S. Eid, Measurement of Hydrogen Produced during Magnesium Corrosion in Hydrochloric Acid and the Effect of the Triton X-100 Surfactant on Hydrogen Production, J. Surfactants Deterg., 2019, 22(1), 153–160.

16 A. Ezzat, et al., Corrosion Inhibition of Carbon Steel in 2.0 M HCl Solution Using Novel Extract (Pulicaria undulate), Biointerface Res. Appl. Chem., 2021, 12(5), 6415–6427.

17 A. Jmiai, et al., A new trend in corrosion protection of copper in acidic medium by using Jujube shell extract as an effective green and environmentally safe corrosion inhibitor: Experimental, quantum chemistry approach and Monte Carlo simulation study, J. Mol. Liq., 2021, 322, 114509.

18 A. Miralrio and A. Espinoza Vázquez, Plant extracts as green corrosion inhibitors for different metal surfaces and corrosive media: a review, Processes, 2020, 8(8), 942.

19 V. Pourzarghan and B. Fazeli-Nasab, The use of Robinia pseudoacacia L fruit extract as a green corrosion inhibitor in the protection of copper-based objects, Heritage Sci., 2021, 9(1), 1–14.

20 A. Al Bahir, Estimation of the performances of creatine and creatinine as eco-friendly corrosion inhibitors for copper in sodium hydroxide solution, *Int. J. Electrochem. Sci.*, 2023, **18**(4), 100040.

21 F. S. de Souza, *et al.*, Adsorption behavior of caffeine as a green corrosion inhibitor for copper, *Mater. Sci. Eng. C*, 2012, **32**(8), 2436–2444.

22 M. Abdallah, *et al.*, Natural occurring substances as corrosion inhibitors for tin in sodium bicarbonate solutions, *J. Korean Chem. Soc.*, 2009, **53**(4), 485–490.

23 S. Mahmoud, Corrosion inhibition of muntz (63% Cu, 37% Zn) alloy in HCl solution by some naturally occurring extracts, *Port. Electrochim. Acta*, 2006, **24**(4), 441.

24 M. Abdallah, *et al.*, Animal glue as green inhibitor for corrosion of aluminum and aluminum-silicon alloys in sodium hydroxide solutions, *J. Mol. Liq.*, 2016, **220**, 755–761.

25 S. Mo, *et al.*, An example of green copper corrosion inhibitors derived from flavor and medicine: vanillin and isoniazid, *J. Mol. Liq.*, 2017, **242**, 822–830.

26 M. Deyab, *et al.*, Experimental and theoretical evaluations on Oleuropein as a natural origin corrosion inhibitor for copper in acidic environment, *Sci. Rep.*, 2022, **12**(1), 7579.

27 M. E. Al-Dokheily, H. M. Kredy and R. N. Al-Jabery, Inhibition of copper corrosion in H2SO4, NaCl and NaOH solutions by Citrullus colocynthis fruits extract, *J. Nat. Sci.*, 2014, **4**(17), 60–74.

28 R. K. Ahmed and S. Zhang, Alchemilla vulgaris extract as green inhibitor of copper corrosion in hydrochloric acid, *Int. J. Electrochem. Sci.*, 2019, **14**(11), 10657–10669.

29 R. M. Abou Shahba, *et al.*, Corrosion and inhibition of Ti-6Al-4V alloy in NaCl solution, *Int. J. Electrochem. Sci.*, 2011, **6**, 5499–5509.

30 R. M. Abou Shahba, *et al.*, Effect of natural products on the corrosion of titanium and its alloy in NaOH solutions, *Int. J. Chem.*, 2012, **4**(1), 30.

31 A. S. Ahmed, *et al.*, The influence of serum bovine and egg albumin on the corrosion of pure aluminum in sodium hydroxide solutions, *Int. J. Appl. Environ. Sci.*, 2012, **7**(3), 289–296.

32 J. Barriga, B. Coto and B. Fernandez, Molecular dynamics study of optimal packing structure of OTS self-assembled monolayers on SiO2 surfaces, *Tribol. Int.*, 2007, **40**(6), 960–966.

33 J. P. Perdew, K. Burke and M. Ernzerhof, Generalized gradient approximation made simple, *Phys. Rev. Lett.*, 1996, **77**(18), 3865.

34 B. Delley, Ground-state enthalpies: evaluation of electronic structure approaches with emphasis on the density functional method, *J. Phys. Chem. A*, 2006, **110**(50), 13632–13639.

35 W. A. Badawy, K. M. Ismail and A. M. Fathi, Corrosion control of Cu–Ni alloys in neutral chloride solutions by amino acids, *Electrochim. Acta*, 2006, **51**(20), 4182–4189.

36 K. M. Ismail, Evaluation of cysteine as environmentally friendly corrosion inhibitor for copper in neutral and acidic chloride solutions, *Electrochim. Acta*, 2007, **52**(28), 7811–7819.

37 M. B. Radovanović, *et al.*, Electrochemical and DFT studies of brass corrosion inhibition in 3% NaCl in the presence of environmentally friendly compounds, *Sci. Rep.*, 2019, **9**(1), 16081.

38 R. Subramanian and V. Lakshminarayanan, Effect of adsorption of some azoles on copper passivation in alkaline medium, *Corros. Sci.*, 2002, **44**(3), 535–554.

39 S. D. Giri and A. Sarkar, Electrochemical study of bulk and monolayer copper in alkaline solution, *J. Electrochem. Soc.*, 2016, **163**(3), H252.

40 J. Ambrose, R. Barradas and D. Shoesmith, Investigations of copper in aqueous alkaline solutions by cyclic voltammetry, *J. Electroanal. Chem. Interfacial Electrochem.*, 1973, **47**(1), 47–64.

41 S. Abd El Haleem and B. G. Ateya, Cyclic voltammetry of copper in sodium hydroxide solutions, *J. Electroanal. Chem. Interfacial Electrochem.*, 1981, **117**(2), 309–319.

42 S. T. Mayer and R. H. Muller, An in situ Raman spectroscopy study of the anodic oxidation of copper in alkaline media, *J. Electrochem. Soc.*, 1992, **139**(2), 426.

43 A. El-Etre, Inhibition of acid corrosion of carbon steel using aqueous extract of olive leaves, *J. Colloid Interface Sci.*, 2007, **314**(2), 578–583.

44 L. Hu, *et al.*, Inhibition effect of TT-LYK on Cu corrosion and galvanic corrosion between Cu and Co during CMP in alkaline slurry, *ECS J. Solid State Sci. Technol.*, 2019, **8**(8), P437.

45 A. A. Khadom and A. S. Yaro, Mass transfer effect on corrosion inhibition process of copper–nickel alloy in hydrochloric acid by Benzotriazole, *J. Saudi Chem. Soc.*, 2014, **18**(3), 214–219.

46 N. Al Otaibi and H. H. Hammud, Corrosion inhibition using harmal leaf extract as an eco-friendly corrosion inhibitor, *Molecules*, 2021, **26**(22), 7024.

47 K. M. Ismail and W. Badawy, Electrochemical and XPS investigations of cobalt in KOH solutions, *J. Appl. Electrochem.*, 2000, **30**, 1303–1311.

48 K. Hladky, L. Callow and J. Dawson, Corrosion rates from impedance measurements: an introduction, *Br. Corros. J.*, 1980, **15**(1), 20–25.

49 J. Hitzig, *et al.*, Frequency response analysis of the Ag/Ag+ system: a partially active electrode approach, *Electrochim. Acta*, 1984, **29**(3), 287–296.

50 N. H. Alharthi, *et al.*, Corrosion inhibition of mild steel by highly stable polydentate schiff base derived from 1, 3-propanediamine in aqueous acidic solution, *J. Saudi Chem. Soc.*, 2022, **26**(4), 101501.

51 E.-D. Wagdy, *et al.*, Inhibition of carbon steel corrosion in aqueous solutions using some fatty amido-cationic surfactant, *J. Basic Environ. Sci.*, 2016, **3**, 55–64.

52 D. F. Seyam, *et al.*, Study of the inhibition effect of two novel synthesized amido-amine-based cationic surfactants on aluminum corrosion in 0.5 M HCl solution, *J. Surfactants Deterg.*, 2022, **25**(1), 133–143.

53 M. A. Abbas, *et al.*, Performance assessment by experimental and Theoretical approaches of newly synthetized benzyl amide derivatives as corrosion inhibitors for carbon steel

in 1.0 M hydrochloric acid environment, *Inorg. Chem. Commun.*, 2022, 109758.

54 M. Bedair, *et al.*, Benzidine-based Schiff base compounds for employing as corrosion inhibitors for carbon steel in 1.0 M HCl aqueous media by chemical, electrochemical and computational methods, *J. Mol. Liq.*, 2020, **317**, 114015.

55 A. H. Ahmed, *et al.*, Ethanedihydrazide as a corrosion inhibitor for iron in 3.5% NaCl solutions, *ACS omega*, 2021, **6**(22), 14525–14532.

56 S. Eid, Expired Desloratidine drug as inhibitor for corrosion of carbon steel pipeline in hydrochloric acid solution, *Int. J. Electrochem. Sci.*, 2021, **16**, 150852.

57 S. Eid, *et al.*, Combination of Experimental and Computational Insight into the Anti-corrosion Performance of 1-(4-tert-butylphenyl)-4-(4-(benzhydryloxy) piperidin-1-yl) butan-1-one onto C-steel in Acidic Environments, *J. Bio- Tribo-Corros.*, 2023, **9**(3), 61.

58 P. Hofmann and A. Rauk, *Orbital Interaction Theory of Organic Chemistry*, Wiley & Sons, New York, 1994, ISBN 0-471-59389-3. 307 Seiten, mit HMO-Programmdiskette, Preis: $45.50. 1995, Wiley Online Library.

59 K. Fukui, Role of frontier orbitals in chemical reactions, *science*, 1982, **218**(4574), 747–754.

60 S. A. Wildman and G. M. Crippen, Prediction of physicochemical parameters by atomic contributions, *J. Chem. Inf. Comput. Sci.*, 1999, **39**(5), 868–873.

61 (*a*) F. J. Luque, J. M. López and M. Orozco, Perspective on "Electrostatic interactions of a solute with a continuum. A direct utilization of ab initio molecular potentials for the prevision of solvent effects, *Theor. Chem. Acc.*, 2000, **103**, 343–345; (*b*) S. Miertus, E. Scrocco and J. Tomasi, *Chem. Phys.*, 1981, **55**, 117; *Theor. Chem. Acc.*, 2000, **103**, 343–345.

62 I. Obot and N. Obi-Egbedi, Adsorption properties and inhibition of mild steel corrosion in sulphuric acid solution by ketoconazole: experimental and theoretical investigation, *Corros. Sci.*, 2010, **52**(1), 198–204.

63 P. Chen, *et al.*, A small disturbance, but a serious disease: The possible mechanism of D52H-mutant of human PRS1 that causes gout, *IUBMB life*, 2013, **65**(6), 518–525.